Int J Mater Form (2008) Suppl 1:1059–1062
DOI 10.1007/s12289-008-0201-2

Determination of the thermophysical properties of a CuCr1Zr alloy from liquid state down to room temperature

J. Wisniewski[1,3], J.-M. Drezet[2], D. Ayrault[3] and B. Cauwe[4]

[1]*LG2M, Université de Bretagne-Sud - 56321 Lorient, France*
URL: www.univ-ubs.fr ; e-mail: jean.wisniewski@gmail.com
[2]*LSMX, Ecole Polytechnique Fédérale de Lausanne - Lausanne, Switzerland*
URL: lsmx.epfl.ch ; e-mail: jean-marie.drezet@epfl.ch
[3]*DEN/DM2S/SEMT/LTA, CEA Saclay - 91191 Gif-sur-Yvette, France*
URL: www.cea.fr ; e-mail: danielle.ayrault@cea.fr
[4]*Le Bronze Industriel - 3 av. du général Leclerc, 51600 Suippes, France*
URL: www.lebronzeindustriel.com ; e-mail: bcauwe@lebronzeindustriel.com

ABSTRACT: Laboratory tests and inverse methods are used for the determination of the thermophysical properties of a CuCrZr alloy. The solidification path (temperature versus solid fraction curve) is determined using the Single Pan Thermal Analysis (SPTA) technique developed at LSMX. The temperature dependent thermal conductivity is identified by inverse analysis using temperature measurements in one dimensional solidified casting. The thermophysical properties will be used as input data in numerical models of the laboratory test aiming at evaluating the hot cracking sensitivity of copper based alloy in electron beam welding for the International Thermonuclear Experimental Reactor (ITER) project.

KEYWORDS: CuCrZr alloy, thermophysical properties, Single Pan Thermal Analysis SPTA, solidification path, thermal conductivity, one dimensional solidified ingot, inverse analysis.

NOMENCLATURE

T_m	Melting temperature of pure copper
m_i	Liquidus slope of alloying element i
k_i	Partition coefficient of alloying element i
c_{0i}	Nominal composition of alloying element i
f_s	Mass solid fraction

1 INTRODUCTION

The precipitation hardened CuCrZr alloy has been selected as a heat sink of the first wall components for the future thermonuclear fusion reactor ITER [1] owing to its good mechanical and thermal properties. The feedback from its use in Tore Supra [2] showed that this alloy is very sensitive to hot tearing (solidification cracking) during electron beam welding. In order to characterize the hot tearing susceptibility of the alloy and thus define acceptance tests of various supplies, a laboratory test, inspired by the work carried out at the Joining and Welding Research Institute (JWRI) [3] is used. An electron beam weld seam is performed on a thin rectangular plate instrumented with thermocouples. The welding parameters (speed and heat input) are fixed. As width of the plate decreases, a crack appears. The test consists in determining this specific width and is analysed with the help of numerical modelling, hot tearing criteria, the local Rappaz-Drezet-Gremaud (RDG) approach [4] and a thermomechanical criteria [5], will be evaluated. To carry out the finite element numerical analysis, it´s necessary to know not only the mechanical behaviour from liquid state down to room temperature but also the thermophysical properties of the alloy. The missing physical properties are determined by associating laboratory tests and numerical analysis.

2 EXPERIMENTAL METHODS

The Single Pan Thermal Analysis (SPTA) is used to determine the solidification path of the CuCr1Zr alloy (EN 12163 CW106C [6]) alloy (Tab. 1).

Table 1: Chemical composition of CuCr1Zr alloy.

Compo. (wt%)	Cu	Cr	Zr	Fe	Si	Other
min	bal.	0.5	0.03	-	-	-
max	bal.	1.2	0.3	0.08	0.1	0.2

Contrary to Differential Thermal Analysis (DTA), SPTA permits the analysis of a huge volume of metal (cm^3 order), thus reducing the effect of nucleation undercooling. Details of this method are available elsewhere [7]. The experiments are conducted with a cylindrical sample (diameter 13.8 mm, height 15 mm) using a high purity gas to minimise oxidation. The samples are subjected to heating and cooling cycles as follows: Room temperature → heating to 1200°C (variable heating rate) → isothermal holding at 1200°C for 3h → cooling (5K/min) to room temperature.

For the determination of the thermal conductivity, cylindrical sample of CuCr1Zr (diameter 40 mm, height 70 mm) is solidified under one dimensional heat flow condition. Fives thermocouples are placed at various distances from the water cooled copper chill (4 mm, 19 mm, 33 mm, 48 mm, and 62 mm). Fig 1 presents the mould and the empty crucible together with the five ceramic tubes in which the thermocouples are inserted. The measured temperature histories are then used in an inverse method to identify the thermal conductivity of the alloy at selected temperatures.

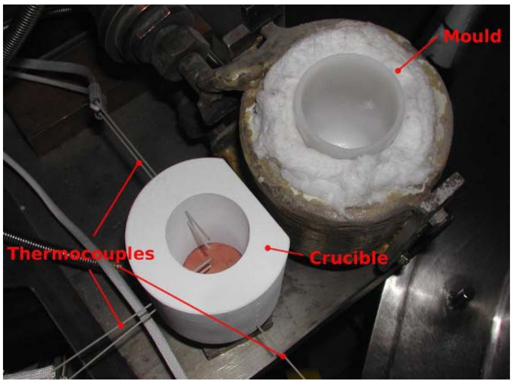

Figure 1: Experimental set up for the 1D casting.

3 RESULTS AND DISCUSSION

3.1 *Solidification path*

Fig 2 shows the solid fraction versus temperature for the CuCrZr alloy obtained by SPTA (cooling rate 5K/min). The liquidus temperature is $T_L = 1080°C$. The slope change of the curve at 1075°C corresponds to the formation of an eutectic phase according to the CuCr binary phase diagram [8].

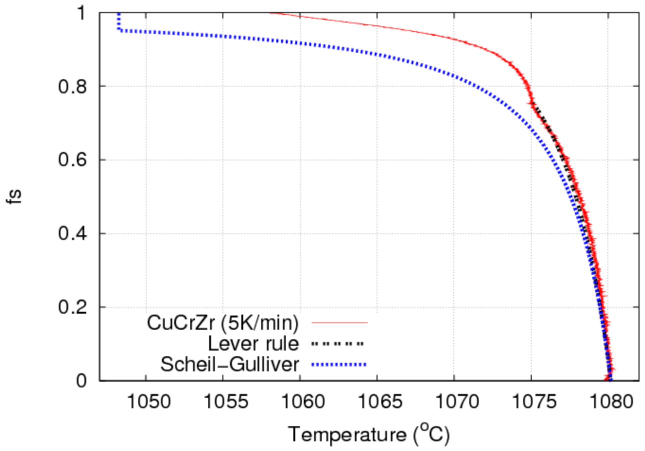

Figure 2: Solidification path of a CuCr1Zr alloy in equilibrium and non equilibrium solidification conditions.

Assuming that the system contains three major elements: chromium, zirconium and phosphorus (deoxidizer), the lever rule is considered [9, 10]:

$$T = T_m + \sum_{i=1}^{3} \frac{m_i c_{0i}}{1-(1-k_i)f_s} \quad (1)$$

This model calculates the solid fraction versus temperature for an equilibrium solidification assuming infinite diffusion in solid and liquid. The coefficients m_i and k_i are unknown. The binary phase diagram of CuCr alloy gives a rough estimation of m_{Cr} and k_{Cr} parameters: $m_{Cr} = -3.5°C/\%wt$ and $k_{Cr} = 0.1$. We consider that the experimental cooling rate (5K/min) is near the cooling rate of equilibrium solidification. Iterative least squares fit is used in order to identify the remaining unknown parameters. The method is based upon a minimization of the error between the calculated $f_s(T)$ curves obtained with the lever rule (1) and the measured curve. The lever rule doesn't take into account the formation of a new phase (i.e. change of slope at 1075°C) so the minimization is led between 1080°C and 1075°C. The obtained values of the coefficients after the minimization are: $m_{Zr} = -5.65°C/\%wt$, $m_P = -5.11°C/\%wt$, $k_{Zr} = 0.1$, $k_P = 0.1$.

In order to obtain the solidification path in quenched conditions, typical conditions encountered during welding, the estimated parameters are used in the Scheil-Gulliver model [9, 10]. This model assumes that there is no solute diffusion in the solid (i.e. the cooling rate is infinite):

$$T = T_m + \sum_{i=1}^{3} m_i c_{0i} (1 - f_s)^{k_i - 1} \qquad (2)$$

Experimental data, lever rule and Scheil-Gulliver model results appear in fig 2.

The problem with the Scheil-Gulliver model is that the lower limit of the solidification interval is not defined. To solve this problem, the fraction of secondary phase is estimated using transverse section of electron beam welding plate. Fig 3 presents scanning electron micrography of a transverse section. Three distinct regions are observed: the base metal (BM), the heat affected zone (HAZ), the melted zone (MZ). Detail of the melted zone is presented in fig 4.

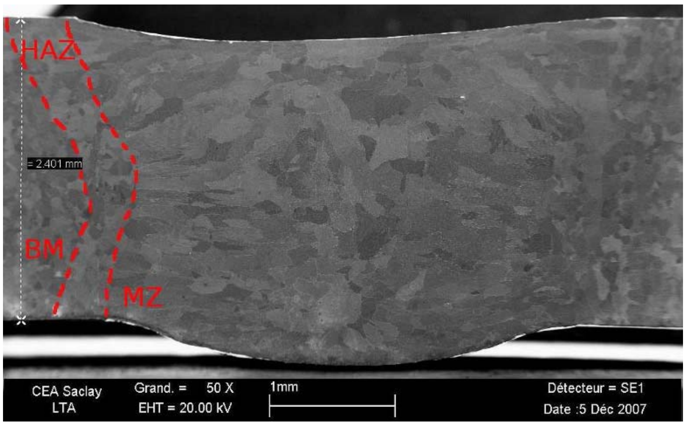

Figure 3: SEM examination of a transverse section of a plate after welding (secondary electrons).

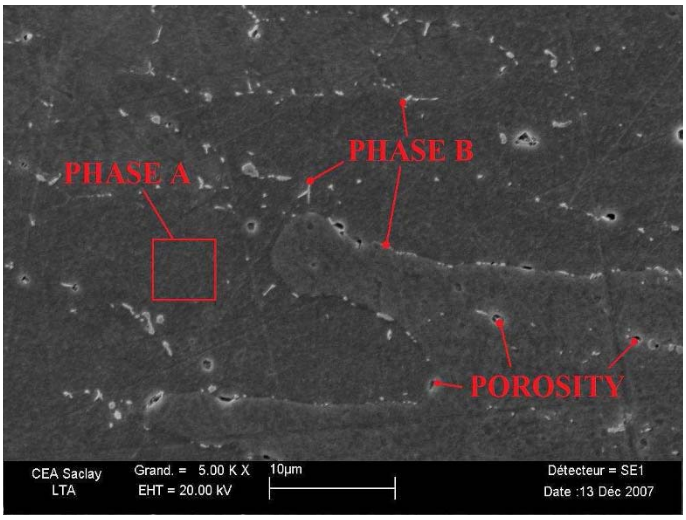

Figure 4: SEM detail within the melted zone.

We mainly observe primary A and secondary B phases and porosity. To determine the volume fraction of each phases, micrographs of the alloy are analysed using the analySIS^{TM} image software. The area fraction is equal to the volume fraction of each phase. Three images were used to calculate the fractions. The image analysis yields a mean value of 5% of secondary phase. Considering the Scheil-Gulliver model, this percentage allow us to fix the non equilibrium solidus temperature at 1048°C (fig 2).

Therefore, the solidification interval is 21°C in equilibrium solidification and 32°C in non equilibrium solidification.

3.2 Thermal conductivity

In order to apply the inverse method described by Rappaz et al [11], the specific heat of CuCrZr presented in fig. 5 is used. For temperatures below 900°C, the data come from [12]. For temperatures greater than 900°C, a linear extrapolation is done. The latent heat of CuCrZr is assumed to be equal to that of pure copper [13]:

$$L_{Cu} = 204 kJ/kg \qquad (3)$$

The result of the inverse calculation is shown in fig. 5. The thermal conductivity of pure copper taken from [13] is also given for comparison.

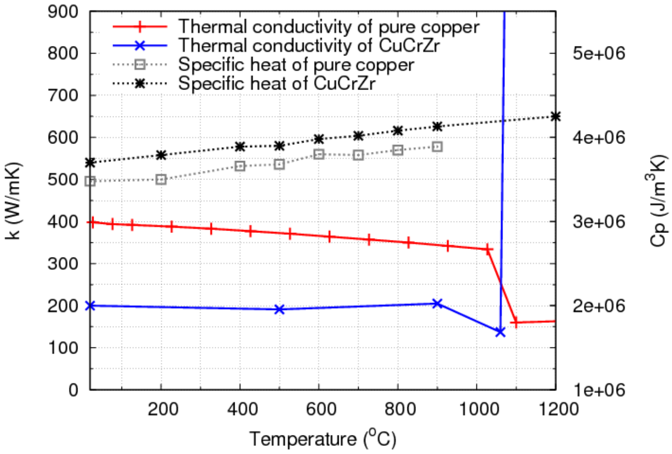

Figure 5: Thermal conductivity and specific heat of a CuCr1Zr alloy and pure copper.

At low temperatures, the thermal conductivity of CuCrZr is two times smaller than the thermal conductivity of pure copper. Indeed, alloying elements decrease the thermal conductivity. In our case, the phenomenon is even more pronounced because Cr and Zr remain in supersaturated solid solution during the fast cooling experienced in the 1D casting. The thermal conductivity of CuCrZr determined in the liquid state is huge owing to the high convection experienced by the liquid metal right after filling the mould (fig 1).

4 CONCLUSIONS

The solidification path and the thermal conductivity are determined for a CuCr1Zr alloy by associating laboratory tests and numerical analysis:

- the solid fraction versus temperature curve is obtained using the single pan thermal analysis (SPTA) technique developed at LSMX. This yields a better description of the solidification path of the alloy not only in equilibrium conditions but also in non-equilibrium conditions as typicaly encountered in electron beam welding.
- the temperature dependent thermal conductivity is deduced from inverse modeling using temperature measurements in one dimensional solidified ingot. It appears that the conductivity is about two times lower than that of pure copper.

ACKNOWLEDGEMENT

The authors express their gratitude to J.-D. Wagnière and F. Kohler who carried out the experiments at the Ecole Polytechnique Fédérale de Lausanne and to F. Castilan for the metallographical inspections at the Laboratoire des Technologies d'Assemblage (LTA-CEA Saclay).

References

[1] U. Luconi, M. Di Marco, A. Federici, M. Grattarola, G. Gualco, J.M. Larrea, M. Merola, C.Ozzano, G. Pasquale. Development of plasma facing components for the dome-liner component of the ITER divertor. *Fusion Engineering and Design*, Vol. 75-79, 2005, pp. 271-276.

[2] M. Lipa, A. Durocher, R. Tivey, Th. Huber, B. Schedler, J. Weigert. The use of copper alloy CuCrZr as a structural material for actively cooled plasma facing and in vessel components. *Fusion Engineering and Design*, Vol. 75-79, 2005, pp. 469-473.

[3] M. Schibahara, H. Serizawa, H. Murakawa. Finite element method for hot cracking analysis using temperature dependent interface element. *Mathematical Modelling of Weld Phenomena*, Vol. 5, 2001, pp. 253-267.

[4] M. Rappaz, J.-M. Drezet and M. Gremaud. A new hot tearing criterion. *Metallurgical and materials transaction A, Vol. 30A, February 1999, pp. 449-445*

[5] N. Kerrouault. Fissuration à chaud en soudage d´un acier inoxydable austénitique. *Thèse CEA-R-5953*, mars 2001.

[6] EN 12163:1998 - number CW106C

[7] F. Kohler, T. Campanella, S. Nakanishi, M. Rappaz. Application of Single Pan Thermal Analysis to Cu-Sn peritectic alloys. *To be published in Acta Materialia*, 2008.

[8] T.B. Massalski, J.L. Murray, L.H. Bennet, H. Baker. Binary Alloy Phase Diagrams Volume 1. *American Society for Metals* 1986.

[9] W. Kurtz, D.J. Fisher. Fundamentals of Solidification, fourth revised edition. *Trans Tech Publications*, 2005.

[10] J.-M. Drezet. Direct Chill and Electromagnetic Casting of Aluminium Alloys: Thermomechanical Effects and Solidification Aspects. *Thesis* 1996.

[11] M. Rappaz, J.-L. Desbiolles, J.-M. Drezet, Ch.-A. Gandinn, A. Jacot and Ph. Thévoz. Application of Inverse Methods to the Estimation of Boundary Conditions and Properties. *Modelling of Casting, Welding and Advanced Solidification Processes VII* 10-15 sept. 1995.

[12] J. Wisniewski, E. Gautier and P. Archambault. Détermination des propriétés thermophysiques et des évolutions microstructurales au cours du chauffage rapide d'un alliage CuCrZr, *Rapport de DEA, Ecole doctorale EMMA*, 2005.

[13] Metals Handbook. Properties and Selection: Nonferrous Alloys and Special Purpose Materials, *ASM International Handbook Commities*.